Available online at www.sciencedirect.com

SCIENCE DIRECT

Virology 351 (2006) 145–158

VIROLOGY

www.elsevier.com/locate/yviro

Comparative mechanistic studies of de novo RNA synthesis by flavivirus RNA-dependent RNA polymerases

Barbara Selisko [a], Hélène Dutartre [a], Jean-Claude Guillemot [a], Claire Debarnot [a], Delphine Benarroch [a], Alexander Khromykh [b], Philippe Desprès [c], Marie-Pierre Egloff [a], Bruno Canard [a,*]

[a] *Centre National de la Recherche Scientifique and Universités d'Aix-Marseille I et II, UMR 6098, Architecture et Fonction des Macromolécules Biologiques, AFMB-CNRS-ESIL, Case 925, 163 avenue de Luminy, 13288 Marseille Cedex 9, France*

[b] *School of Molecular and Microbial Sciences, The University of Queensland, Brisbane QLD, 4072, Australia*

[c] *Institut Pasteur, Interactions Moléculaires Flavivirus-Hôtes, Institut Pasteur, 75724 Paris, France*

Received 27 January 2006; returned to author for revision 22 February 2006; accepted 16 March 2006

Available online 21 April 2006

Abstract

Flavivirus protein NS5 harbors the RNA-dependent RNA polymerase (RdRp) activity. In contrast to the RdRps of hepaci- and pestiviruses, which belong to the same family of *Flaviviridae*, NS5 carries two activities, a methyltransferase (MTase) and a RdRp. RdRp domains of Dengue virus (DV) and West Nile virus (WNV) NS5 were purified in high yield relative to full-length NS5 and showed full RdRp activity. Steady-state enzymatic parameters were determined on homopolymeric template poly(rC). The presence of the MTase domain does not affect the RdRp activity. Flavivirus RdRp domains might bear more than one GTP binding site displaying positive cooperativity. The kinetics of RNA synthesis by four *Flaviviridae* RdRps were compared. In comparison to Hepatitis C RdRp, DV and WNV as well as Bovine Viral Diarrhea virus RdRps show less rate limitation by early steps of short-product formation. This suggests that they display a higher conformational flexibility upon the transition from initiation to elongation.

Keywords: Dengue virus; Hepatitis C virus; Flavivirus; *Flaviviridae*; RdRP; Pestivirus; Polymerase; RNA synthesis; West Nile virus

Introduction

The *Flaviviridae* virus family comprises three genera of single-stranded positive-sense RNA viruses: hepaciviruses (Hepatitis C virus (HCV)), pestiviruses (e.g., Bovine Viral Diarrhea virus (BVDV)) and flaviviruses (e.g., Dengue virus (DV) and West Nile virus (WNV)). The genus flavivirus contains at least 70 mosquito-borne or tick-borne viruses. DV threatens up to 2.5 billion people in 100 endemic countries (Mackenzie et al., 2004). Between 50 and 100 million cases of dengue fever occur annually with 500,000 cases of the severe disease form dengue hemorrhagic fever, and 22,000 deaths mainly among children (Guzman and Kouri, 2002). Dengue has been classified a priority by the World Health Organization (WHO). It ranks as the most important mosquito-borne viral disease in the world (http://www.who.int/csr/disease/dengue). WNV was first isolated in Africa in 1937 and showed an extensive distribution throughout the world except in the Americas (Mackenzie et al., 2004). In 1999, a first WNV outbreak occurred in New York City. By the end of 2003, WNV activity had been identified in 46 states of the United States. In 2005 (until October, 18), WNV epidemics resulted in 2,316 reported cases of WN disease including 913 meningitis or encephalitis cases and 66 deaths (http://www.cdc.gov/ncidod/dvbid/westnile/). Kunjin virus (KV) is an Australian subtype of WNV (Scherret et al., 2001). In contrast to other WNV strains (Lanciotti et al., 2002), KV infections do not cause neuroinvasive disease in humans (Hall et al., 2002).

* Corresponding author. Fax: +33 491 828646.
E-mail address: Bruno.Canard@afmb.univ-mrs.fr (B. Canard).

0042-6822/$ - see front matter © 2006 Elsevier Inc. All rights reserved.
doi:10.1016/j.virol.2006.03.026

Currently, there is no specific treatment available for DV or WNV infections. Different approaches towards efficient vaccines are under development (Hall and Khromykh, 2004; Hall et al., 2003; Pugachev et al., 2003). Apart from the vaccine approach and vector control measurements, antibody-based (Roehrig et al., 2001) and antiviral drug therapies might be considered relevant for future control of DV and WNV infections.

Viral RNA-dependent RNA polymerases (RdRps) represent targets of choice for anti-viral chemotherapy. They are essential to viral replication and present a unique evolutionary fate of being the only replicative RdRps preserved from the RNA world (Leipe et al., 1999). *Flaviviridae* RdRp duplicates the single-stranded flavivirus RNA genome in a single, continuous polymerization event. The RdRp enters at the 3′-end of the genome and is able to copy the whole RNA molecule in a primer-independent fashion (Bressanelli et al., 2002; Kao et al., 2001), referred to as *de novo* RNA synthesis. Viral RdRps belong to the SCOP (Structural Classification Of Proteins (Murzin et al., 1995)) superfamily of DNA/RNA polymerases. Crystal structures of various viral RdRps have been reported, among them that of two *Flaviviridae*, HCV and BVDV (Ago et al., 1999; Bressanelli et al., 1999, 2002; Choi et al., 2004; Lesburg et al., 1999). Their overall shape resembles a right hand with three subdomains: the "fingers", the central catalytic "palm" subdomain containing at least two strictly conserved acidic residues responsible for binding two catalytic Mg^{2+} ions, and the "thumb". The crystal structure of BVDV RdRp has shown interesting structural differences relative to that of HCV RdRp namely in a specific thumb region (named "β-hairpin" or "flap" for HCV RdRp and "β-thumb" region for BVDV RdRp) which is believed to play a role in the initiation of de novo RNA synthesis. Thus, although viruses of the *Flaviviridae* family have similar genome organization and replication mechanisms, these similarities do not necessarily translate into homologies at the molecular level.

The largest non-structural protein NS5 of flaviviruses harbors the RdRp activity. Signature-sequence analysis suggests that NS5 is made of two domains separated by an ill-defined inter-domain region. The three-dimensional structure of a N-terminal domain of 30 kDa of DV has been determined (Egloff et al., 2002). It bears a (nucleoside-2′-O-)-methyltransferase (MTase) activity involved in the formation of the type-1 cap of genomic RNA, unique to flaviviruses in contrast to pestiviruses and hepaciviruses. Accordingly, RdRps of HCV and BVDV, named NS5B, do not contain a MTase domain. The DV MTase domain ($NS5MTase_{DV}$) domain is able to bind GTP as well as GTP analogues, such as ribavirin 5′-triphosphate, a broad-spectrum inhibitor of viral replication (Benarroch et al., 2004). A C-terminal domain of ca. 70 kDa harbors the RdRp, as judged by the presence of signature-sequence motifs A to F (Koonin, 1991; O'Reilly and Kao, 1998). The crystal structure of the RdRp domain is not known. Two nuclear localization sequences (bNLS from amino acid 320 to 369 and a/bNLS from 370 to 405) are thought to map in the inter-domain region (Brooks et al., 2002).

Full-length NS5 of DV ($NS5_{DV}$) and WNV ($NS5_{WNV}$) have been obtained from *E. coli* expression systems (Ackermann and Padmanabhan, 2001; Nomaguchi et al., 2004; Tan et al., 1996) and baculovirus/insect cell expression systems (Guyatt et al., 2001; Steffens et al., 1999). The number of enzymatic studies of flavivirus RdRps is still limited and reports contradictory results. $NS5_{DV}$ and $NS5_{WNV}$ were shown to be active on specific subgenomic RNA templates of positive and negative polarity (Ackermann and Padmanabhan, 2001; Nomaguchi et al., 2004), whereas in the same study, enzymatic activity on unspecific heteropolymeric templates was virtually undetectable. In contrast, another report showed that recombinant $NS5_{KV}$ was active on an unspecific heteropolymeric RNA (Guyatt et al., 2001). Recombinant $NS5_{WNV}$ present in insect cell extracts was reported to be active on homopolymeric RNA templates (poly(rC)) but exclusively in the presence of an oligo $(rG)_{18}$ primer (Steffens et al., 1999). On subgenomic RNA templates, $NS5_{DV}$ and $NS5_{WNV}$ were able to initiate polymerization de novo generating a template-size product (Ackermann and Padmanabhan, 2001; Nomaguchi et al., 2004). Products twice the template size were also observed originating presumably from a copy-back mechanism. In the copy-back mechanism, templates adopt a hairpin conformation due to the existence of short complementary sequence stretches in the 3′ region. The 3′-end hybridizes internally and is then elongated. Copy-back elongation is considered unique to in vitro experimental conditions whereas de novo initiation is thought to be the mechanism used in infected cells during *Flaviviridae* virus replication (Bressanelli et al., 2002; Kao et al., 2001). For RNA synthesis by $NS5_{DV}$ on a negative-sense subgenomic template, the ratio of de novo versus copy-back products increases when the temperature during initiation is lowered. Consequently, a model was proposed where the enzyme adopts a closed conformation around the 3′ of the template in the initiation complex and then opens up for elongation (Ackermann and Padmanabhan, 2001). De novo RNA synthesis requires unusually high GTP concentrations in comparison to

Fig. 1. Structure-based sequence alignment of RdRp domains of NS5 of DV (DV_2_NGC) and WNV (strain IS-98-ST1 (WNV_IS98ST1) and Kunjin subtype, strain MRM61C (WNV_Kunjin)) and single-domain RdRps NS5B of HCV and BVDV. Residue numbering corresponds to full-length $NS5_{DV}$. Secondary-structure prediction for $NS5Pol_{DV}$ done by PredictProtein (Rost, 1996) is shown above the alignment. Secondary structural elements of $NS5B_{HCV}$ and $NS5B_{BVDV}$ (Choi et al., 2004; Lesburg et al., 1999) are shown below. The sequence of $NS5B_{BVDV}$ starts with the first residue considered to belong to the RdRp core (Choi et al., 2004). RdRp subdomains (fingers—blue, palm—green, thumb—orange) are indicated by colored lines above the alignment. Motifs A to F are shown by red bars below the alignment. Strictly conserved residues within *Flaviviridae* family RdRps are given in white on a red background. Two NLSs (bNLS and a/bNLS) present only in flavivirus RdRps are delineated by red rectangles in the predicted secondary structure line. Alignment was generated by comparison of the two structures using Swiss-Prot PDB viewer (http://www.expasy.org/spdbv/) and the flavivirus sequences were then aligned manually using Seaview (Galtier et al., 1996). Graphic visualization was generated by Espript (Gouet et al., 2003).

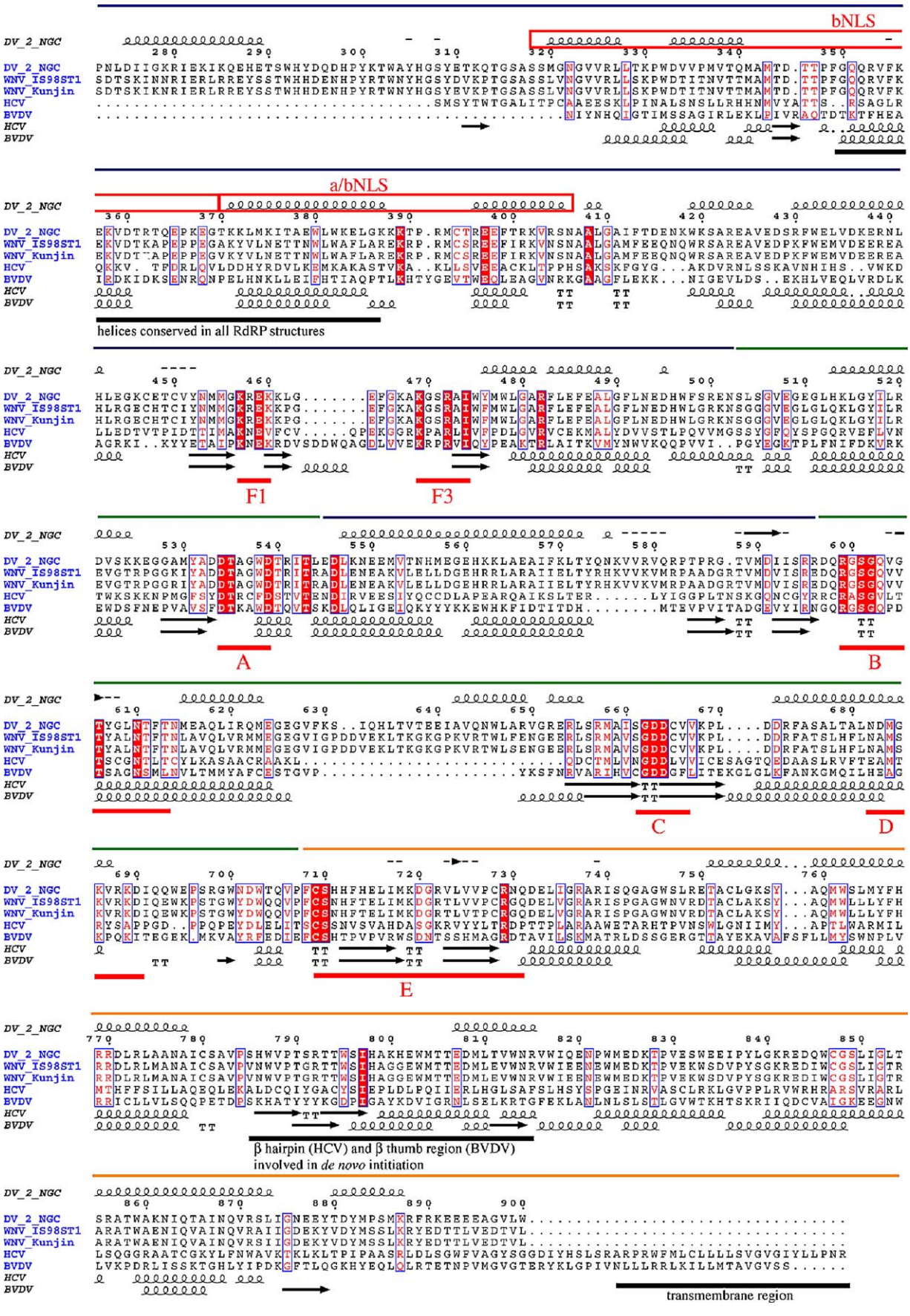
bNLS
a/bNLS
DV_2_NGC
WNV_IS98ST1
WNV_Kunjin
HCV
BVDV
HCV
BVDV
helices conserved in all RdRP structures
F1
F3
A
B
C
D
E
β hairpin (HCV) and β thumb region (BVDV)
involved in de novo intitiation
transmembrane region

other NTPs (Nomaguchi et al., 2003). For all flaviviruses, GTP is the second nucleotide to be incorporated during negative-sense and positive-sense RNA synthesis. GTP might play a special role in the RNA synthesis initiation process. Two hypothesis were discussed: (1) that GTP is in fact the initiating nucleotide for negative-strand synthesis or (2) that GTP has a conformational effect, i.e., a putative allosteric GTP binding site has to be occupied to allow the enzyme to adopt the closed conformation for de novo initiation (Nomaguchi et al., 2003). The K_m value for GTP could not be measured for de novo RNA synthesis because the effect of increasing GTP concentration did not follow Michaelis–Menten kinetics (Nomaguchi et al., 2003). The authors suggested that the existence of the above-mentioned GTP binding site on the N-terminal MTase domain of NS5 might be a reason. The separation of the two domains of flavivirus NS5 and thus the dissociation of their activities is expected to contribute to the precise characterization of the enzymatic activity of NS5.

Here, we report, for the first time, a characterization of functional recombinant flavivirus RdRp domains, NS5Pol, of DV and WNV regarding their RNA polymerization mechanism.

Results

Much of the current knowledge on *Flaviviridae* RdRps is derived from pestivirus (BVDV) and hepacivirus (HCV) RdRps. Relative to HCV and BVDV RdRps, substrate binding and kinetic analysis of flavivirus NS5 bearing the RdRp function is complicated by the presence of an additional nucleotide-, RNA-, and S-adenosyl-L-methionine-binding MTase domain presumably involved in RNA capping. We have performed a detailed comparative kinetic analysis of flavivirus RdRp domains and full-length NS5 in order to derive mechanistic insights useful to future anti-flavivirus drug design. In the absence of flavivirus RdRp structural data, we made use of HCV and BVDV RdRp crystal structures (Ago et al., 1999; Bressanelli et al., 1999, 2002; Choi et al., 2004; Lesburg et al., 1999) to correlate flavivirus RdRp kinetics to existing *Flaviviridae* functional and structural data.

Flavivirus RdRp domain delineation, protein expression and purification

Based on previous structural and functional studies on the MTase domain of DV NS5 ($NS5MTase_{DV}$) (Egloff et al., 2002), we defined several putative functional and soluble C-terminal RdRp domains of $NS5_{DV}$ starting before and after the nuclear localization sequences (NLS). One of them proved to be over-expressed in *E. coli*, in a soluble and stable fashion. It starts at amino acid Pro272 for $NS5Pol_{DV}$ (corresponding to Ser274 for $NS5Pol_{WNV}$ and $NS5Pol_{KV}$), thus just after the ordered part (amino acids 1 to 264) seen in the $NS5MTase_{DV}$ crystal structure (Egloff et al., 2002). The two NLS belong to this construct (Fig. 1). Fig. 1 shows a structure-based sequence alignment of the RdRp domains of DV and WNV with the RdRps NS5B of HCV and BVDV showing the secondary structure predicted for $NS5Pol_{DV}$ by the PredictProtein server (Rost, 1996) and the actual secondary structures of the RdRps of HCV (Lesburg et al., 1999) and BVDV (Choi et al., 2004). Flavivirus RdRp domains share 34% of sequence identity (comparison conducted with tick-borne and mosquito-borne flaviviruses compiled in the Viral Enzyme Module Localization Database VazyMolO (Ferron et al., 2005b) except Cell fusing agent virus, Kamiti River virus and Tamana bat virus). Considerably less sequence identity is shared between *Flaviviridae* RdRps. The alignment in Fig. 1 renders only 3% identical residues. These conserved residues are mainly limited to motif F in the finger subdomain and the catalytic residues of motifs A to C within the palm subdomain as well as motif E in the transition zone between palm and thumb subdomains. The least conserved subdomain among *Flaviviridae* RdRps is the thumb domain. In the case of the RdRps of HCV ($NS5B_{HCV}$) and BVDV ($NS5B_{BVDV}$), it provides structural elements essential for de novo initiation (indicated in Fig. 1) (Bressanelli et al., 2002; Choi et al., 2004). The C-terminus of flavivirus NS5 does not contain a hydrophobic stretch used as a membrane anchor as in the case of $NS5B_{HCV}$ and $NS5B_{BVDV}$ (Fig. 1).

We then expressed and purified the RdRp domains $NS5Pol_{DV}$ (DV, type 2, strain New Guinea C), $NS5Pol_{WNV}$ (WNV, strain IS-98-ST1), and $NS5Pol_{KV}$ (WNV, subtype Kunjin, strain MRM61C) as well as full-length $NS5_{DV}$ and $NS5_{KV}$. Proteins were expressed with an N-terminal His_6-tag. Average yields after the first purification step and final yields are given in Table 1. Expression is generally stronger for WNV proteins. The expression vector is irrelevant as a construct of $NS5_{DV}$ in the expression vector pDest14 (used throughout for the expression of WNV proteins) rendered low expression levels. Additionally, after expression, DV proteins are more difficult to solubilize than WNV proteins. The yield of RdRp domains was always considerably higher than that of full-length NS5. As an example, expression and purification of $NS5Pol_{DV}$ and $NS5_{DV}$ is given in Figs. 2A and B, respectively. Fig. 2C shows all proteins used in this study after a two-step purification protocol.

Flavivirus RdRp activity tests and optimization studies

Enzymatic activity was first tested for $NS5Pol_{DV}$ using a heteropolymeric specific template (RNA minigenome) containing the 5′-end (224 nucleotides) fused to the 3′-end (492 nucleotides) of the DV genomic RNA sequence (Fig. 3A). The main product consists in a hairpin product, twice the size of the

Table 1
Purification yields of recombinant NS5 RdRp domains NS5Pol of DV and WNV (strain IS-98-ST1 (WNV) and Kunjin subtype, strain MRM61C (KV)) as well as full-length proteins NS5

RdRp	$NS5Pol_{DV}$	$NS5_{DV}$	$NS5Pol_{WNV}$	$NS5Pol_{KV}$	$NS5_{KV}$
Yield after IMAC (mg/l culture)	2.6	1.0	8.0	5.0	4.2
Final yield (mg/l culture)	1.0	0.2	3.0	2.0	0.4

Proteins were expressed with a N-terminal His_6-tag and purified as described in Materials and methods.

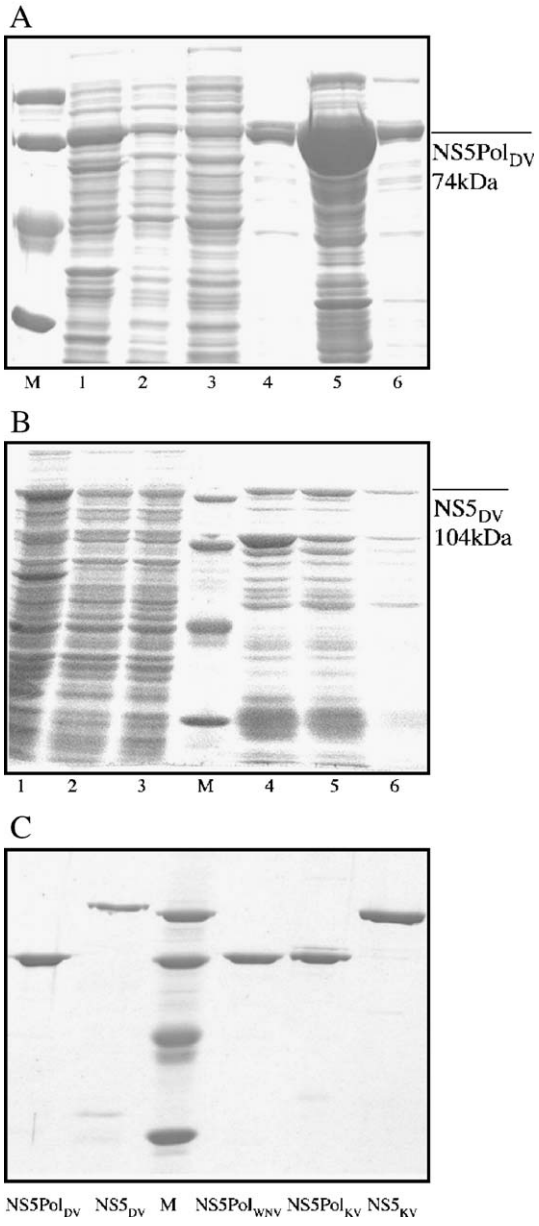

Fig. 2. Expression and purification of RdRp domains NS5Pol and full-length NS5 proteins of DV and WNV (strain IS-98-ST1 (WNV) and subtype Kunjin strain MRM61C (KV)). (A) SDS-PAGE purification profile of NS5Pol$_{DV}$. Lane 1: total protein fraction of cell lysate, lane 2: soluble fraction, lane 3: unbound protein fraction after applying the soluble fraction to the Co^{2+} affinity-chromatography resin, lanes 4 to 6 eluted fraction from Co^{2+} affinity chromatography. M: low-molecular weight marker corresponding to 94, 67, 43 and 30 kDa. (B) SDS-PAGE purification profile of NS5$_{DV}$. Lanes as in panel A, applied quantities were normalized according to the volume of cell culture processed for NS5Pol$_{DV}$ and NS5$_{DV}$. (C) Purified proteins after two-step purification. The identity of each protein is given below. M: low-molecular weight marker as in panel B.

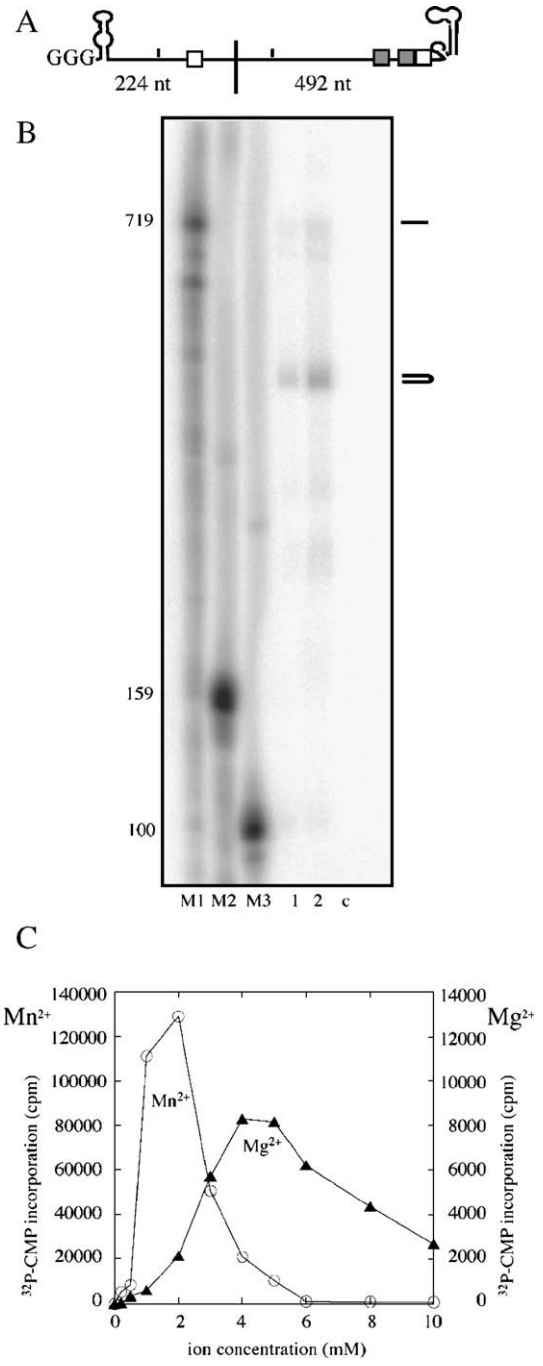

Fig. 3. RNA synthesis by NS5Pol$_{DV}$ on heteropolymeric template (Dengue minigenome). (A) Schematic representation of the template consisting of the first 224 nucleotides of the 5′-end of Dengue genomic RNA including the 5′ cyclization sequence (white square) within the coding sequence (starting after the vertical bar) of the C protein and the last 492 nucleotides of the 3′-end including the complementary 3′ cyclization sequence (white square) and two consensus sequence stretches (grey squares). (B) PAGE visualization of RNA-synthesis products. Reaction mixtures containing 50 nM (lane 1) and 100 nM (lane 2) NS5Pol$_{DV}$ were set up as described under Materials and methods. Labeled template was used as RNA size marker (M1) as well as unrelated RNA molecules of 159 (M2) and 100 nucleotides (M3). A control reaction was included with 100 nM NS5MTase$_{DV}$ (c). (C) Mn^{2+} and Mg^{2+} concentration optima for RNA synthesis. Reaction mixtures were set up as described under Materials and methods. [^{32}P]-CMP incorporation (counts per minute) after 60 min in presence of Mn^{2+} (○) or Mg^{2+} (▲) was detected by filter-binding and liquid scintillation counting and plotted against cation concentration.

template, which is expected to derive from elongation at the 3′-end (copy-back mechanism). As reported by others (You and Padmanabhan, 1999), this product migrated faster in a polyacrylamide gel (Fig. 3B) than the template-sized product, which was also observed. Its apparent size of 1430 nucleotides was confirmed in a formaldehyde-agarose gel where the hairpin product is fully dissociated (not shown). NS5Pol$_{DV}$ activity

supported Mg^{2+} or Mn^{2+} as catalytic ions. The optimum concentrations of both ions were determined (Fig. 3C). CMP-incorporation is around 15-fold higher in the presence of Mn^{2+} at its optimum concentration of 2.0 mM than in the presence of Mg^{2+} at its optimum concentration of 4.5 mM.

The activity of the whole series of produced flavivirus RdRp proteins was then tested on homopolymeric RNA template poly (rC) in the presence or absence of a small rGG primer. All preparations are able to incorporate labeled [^{3}H]-GMP into a putative poly(rG) product regardless of the presence of the small primer. Thus, all RdRps are able to perform de novo initiation. There is no evidence that enzymes use the small primer. GMP incorporation was essentially the same with and without rGG (not shown) in the reaction mixture. A typical time course of GMP incorporation into a poly(rG) product using poly(rC)/rGG is shown in Fig. 4A for $NS5Pol_{DV}$ and $NS5_{DV}$. It can be described with the exponential equation $P = P_{max}(1-e^{-kt})$, P being the generated product measured in counts per minute (cpm), P_{max} the maximum amount of product formed during the reaction, k the pseudo-first order rate constant and t the reaction time. In a control assay, the specific *E. coli*-DdRp inhibitor rifampicin is added and does not cause any inhibition of the RdRp activity observed with $NS5Pol_{DV}$ and $NS5_{DV}$. In contrast, the RdRp activity on poly(rC)/rGG of *E. coli* DdRp used as a control enzyme is inhibited. Thus, we exclude contamination of the recombinant RdRps with *E. coli* DdRp. Fig. 4B illustrates the incorporation of [α-^{32}P]-GMP by $NS5Pol_{DV}$ into long product chains (indicated by an arrow on the top-right of the gel) during 15 min. Even after 1 min, a considerable amount of apparently full-length product is formed. Note that a considerable amount of this product is retained in the wells; only a low percentage migrates according to its expected average size of 500 nucleotides. This is due to the tendency of poly(rG) to form higher structures. In the lower part of the gel, two abortive products G_2 and G_4 accumulate during the polymerization reaction (indicated by arrows on the right). Visualization of the polymerization reaction by $NS5_{DV}$ and $NS5Pol_{WNV}$ using poly (rC) as a template showed comparable results of full-length

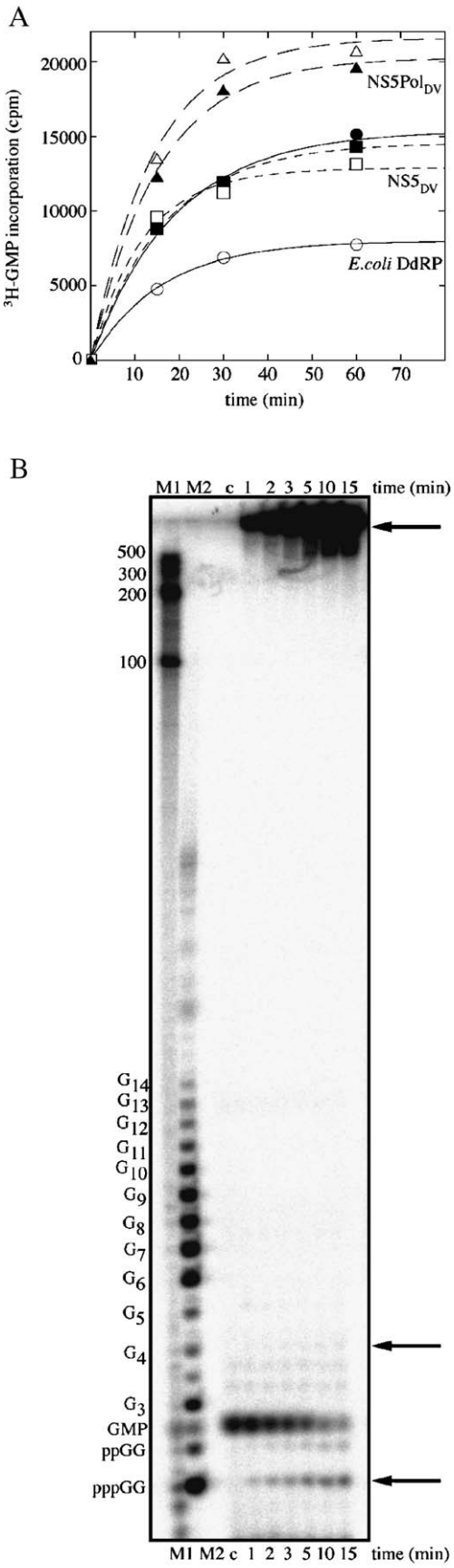

Fig. 4. RNA synthesis by $NS5Pol_{DV}$ and $NS5_{DV}$ on homopolymeric RNA template poly(rC). Reaction mixtures containing enzyme at concentrations given below, 1 μM poly(rC) RNA template and 10 μM GTP were set up as described under Materials and methods. (A) Time course of [^{3}H]-GMP incorporation on poly(rC)/rGG by $NS5Pol_{DV}$ (60 nM, ▲, △), $NS5_{DV}$ (40 nM, ■, □) and *E. coli* DdRp (37 nM, ●, ○) in absence (closed symbols) or presence (open symbols) of *E. coli* DdRp inhibitor rifampicin monitored by filter-binding and liquid scintillation counting. Reaction was followed up to 60 min. Data were fitted to the exponential equation $P = P_{max}(1-e^{-kt})$, P being the generated product measured in counts per minute (cpm), P_{max} the maximum amount of product formed during the reaction, k the pseudo-first order rate constant and t the reaction time. (B) Time course of [α-^{32}P]-GMP incorporation on 1 μM poly(rC) using 10 μM [α-^{32}P]-GTP and 60 nM $NS5Pol_{DV}$. RNA products were resolved on a 14% polyacrylamide denaturating gel. M1 (lane 1): RNA size marker. M2 (lane 2): Oligo(rG) RNA synthesized by T7 DdRp used as RNA size marker (indicated on the left). c: Control reaction mixture without enzyme. Time course of reaction was followed up to 15 min. The presence of short (pppGG and G_4) and template-size reaction products are indicated on the right by arrows. GMP is generated from GTP by heating the aliquots before migration to 95 °C during 7 min, its concentration decreases as GTP is used in the reaction.

product formation with minor amounts of small abortive products (not shown).

As RdRp reaction buffer we used 50 mM HEPES at pH 8.0 with 10 mM KCl and 10 mM DTT. KCl and DTT were tested to be beneficial for RdRp activity at these concentrations (not shown). In RdRp reaction mixtures, non-ionic detergents are often used at low concentrations. We tested the effect of triton X-100 on our enzymes at 0.1%. Likewise, the effect of the presence of BSA as a stabilizing agent during the reaction was tested at 10 μg/ml and 100 μg/ml. Surprisingly, in the presence of 0.1% triton NS5Pol$_{DV}$ showed only 49.3% activity and NS5Pol$_{KV}$ 22.0%. Similar values were found for full-length proteins. At 10 μg/ml BSA 96% to 100% activity was detected. All three enzymes did not support the presence of 100 μg/ml BSA. NS5Pol$_{DV}$ retained 15.7% of its activity, NS5Pol$_{WNV}$ and NS5Pol$_{KV}$ lost their activity almost completely. Subsequent tests were conducted in absence of detergent and BSA.

In contrast to the RNA synthesis on a specific heteropolymeric template (see above), RNA polymerization on poly (rC) was detected only when Mn^{2+} ions are present in the reaction mixture. The optimal Mn^{2+} concentration as single divalent cation present in the reaction and in presence of 5 mM Mg^{2+} ions were determined for NS5Pol$_{DV}$ and NS5Pol$_{WNV}$ (Fig. 5). Concentration optima for Mn^{2+} are 3 mM for both enzymes, and shift towards 5 mM in the presence of Mg^{2+}. NS5Pol$_{WNV}$ tolerates higher concentrations of Mn^{2+} than NS5Pol$_{DV}$. Hence, the following experiments on homopolymeric templates were performed in the presence of both 5 mM Mn^{2+} and 5 mM Mg^{2+}.

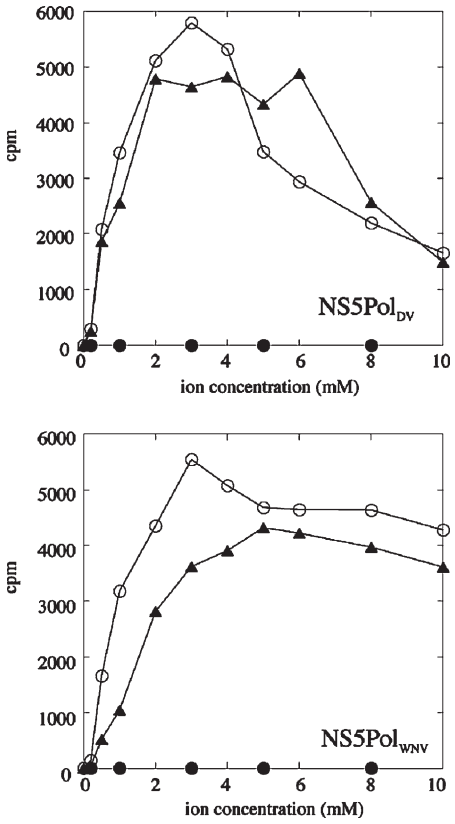

Fig. 5. Mn^{2+} concentration optima of NS5Pol$_{DV}$ and NS5Pol$_{WNV}$ for RNA synthesis on homopolymeric RNA template poly(rC). Reaction mixtures containing enzyme (60 nM NS5Pol$_{DV}$, 400 nM NS5Pol$_{WNV}$), 1 μM poly(rC) RNA template and GTP (10 μM for NS5Pol$_{DV}$ and 100 μM for NS5Pol$_{WNV}$) were set up as described under Materials and methods. [^{3}H]-GMP incorporation (counts per minute) after 10 min in presence of Mn^{2+} (○), Mg^{2+} (●) or Mn^{2+} in presence of 5 mM Mg^{2+} (▲) was detected by filter-binding and liquid scintillation counting and is plotted against cation concentration.

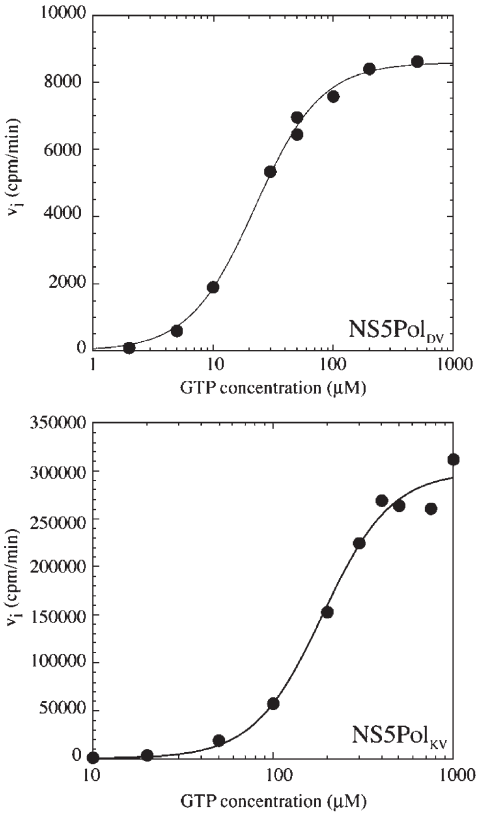

Fig. 6. Steady-state kinetics of NS5Pol$_{DV}$ and NS5Pol$_{KV}$ for de novo RNA synthesis on homopolymeric RNA template poly(rC). Reaction mixtures containing enzyme (40 nM NS5Pol$_{DV}$, 150 nM NS5Pol$_{KV}$), 1 μM poly(rC) RNA template and increasing concentrations of GTP were set up as described under Materials and methods. Reactions were followed up to 4 min. [^{3}H]-GTP incorporation (counts per minute) was monitored by filter-binding and liquid scintillation counting. Initial velocities (cpm per min) were calculated by linear regression and plotted against corresponding GTP concentrations. To show the sigmoid shape of the curve, GTP concentration was plotted in logarithmic scale. Data were fitted using the Hill equation, $v_i = V_{max}[GTP]^h / ((K_{0.5})^h + [GTP]^h)$ with V_{max} being the maximum velocity in cpm per min, $K_{0.5}$ the substrate concentration at $V_{max}/2$ and h the Hill coefficient. Hill coefficients and $K_{0.5}$ values are given in Table 2.

Steady-state kinetic constants on homopolymeric RNA templates

K_m values for GTP as a substrate were determined using poly (rC) without rGG primer (de novo RNA synthesis). Enzymes were tested within a concentration range of 20 to 150 nM where the initial velocity is linearly proportional to the enzyme concentration (not shown). The template poly(rC) was used at 1 μM throughout. This is a saturating concentration. Keeping GTP concentration at 200 μM, we attempted to characterize

saturation with lower concentrations and this suggested apparent K_m values of poly(rC) of less than 40 nM. Full characterization of a saturation curve would have required enzyme concentrations too small for accurate measurements. Initial velocities were measured for different GTP concentrations and used to determine K_m(GTP) values. Curve-fitting was considerably better using the Hill equation: $v_i = V_{max}[GTP]^h / ((K_{0.5})^h + [GTP]^h)$ with V_{max} being the maximum velocity in cpm per min, $K_{0.5}$ the substrate concentration at $V_{max}/2$ and h the Hill coefficient, than when a classic Michaelis–Menten equation (Hill coefficient set to 1) was used. In the latter case $K_{0.5}$ turns into K_m, both having the same meaning. Figs. 6A and B illustrate the fit to sigmoidal Hill equations for $NS5Pol_{DV}$ and $NS5Pol_{KV}$, respectively. Table 2 shows $K_{0.5}$ values and Hill coefficients. Concerning the $K_{0.5}$ values, WNV NS5 proteins presented significantly higher values for $K_{0.5}$ in comparison to DV NS5 (5 to 8-fold). The Hill coefficients varied between 1.6 and 2.7. The observed differences between WNV and KV RdRps were judged to lie within the range of experimental variation. Thus, we conclude that all flavivirus RdRps show a Hill coefficient greater than 1. Finally, for both Hill coefficients and $K_{0.5}$(GTP), NS5 RdRp domains and full-length proteins showed similar values. This was also observed for the calculated k_{cat} values of WNV RdRp constructs of 1635, 2820 and 1983 cpm/s pmol enzyme for $NS5Pol_{WNV}$, $NS5Pol_{KV}$ and $NS5_{KV}$, respectively. Concerning the DV proteins we calculated k_{cat} values 2364 and 945 cpm/s pmol for $NS5Pol_{DV}$ and $NS5_{DV}$, respectively.

Additionally, poly(rA) and poly(rU) were tested as alternative templates. We determined the percentage of initial velocity (cpm/min) of [^{3}H]-NMP incorporation in comparison to poly(rC) keeping the same reaction conditions (100 μM NTP and 1 μM template concentration). $NS5Pol_{DV}$ and $NS5_{DV}$ showed activity using poly(rU) corresponding to 13% and 33% of initial velocity, respectively. No activity was detected using poly(rA). WNV RdRps did not use poly(rA)/UTP nor poly(rU)/ATP as template/nucleotide systems. Here again, RdRp domains and full-length proteins showed an identical behavior.

Table 2
Steady-state kinetics of flavivirus NS5Pol and NS5 proteins for de novo RNA synthesis on homopolymeric RNA template poly(rC)

RdRp	$NS5Pol_{DV}$	$NS5_{DV}$	$NS5Pol_{WNV}$	$NS5Pol_{KV}$	$NS5_{KV}$
$K_{0.5}$ GTP (μM)	22.5 ± 1.1	11.4 ± 2.0	271.8 ± 65.2	188.8 ± 14.8	113.0 ± 9.6
Hill coefficient	1.6 ± 0.1	1.6 ± 0.4	1.6 ± 0.4	2.3 ± 0.3	2.7 ± 0.7

Reaction mixtures containing enzyme (40 nM to 135 nM), 1 μM poly(rC) RNA template and increasing concentrations of GTP were set up as described under Materials and methods. Reactions were followed up to 4 min. [^{3}H]-GTP incorporation (counts per minute) was monitored by filter-binding and liquid scintillation counting. Initial velocities (cpm per min) were calculated by linear regression and plotted against corresponding GTP concentrations. Data were fitted using the Hill equation, $v_i = V_{max}[GTP]^h / ((K_{0.5})^h + [GTP]^h)$ with V_{max} being the maximum velocity in cpm per min, $K_{0.5}$ the substrate concentration at $V_{max}/2$ and h the Hill coefficient. Results of one of two independent test series are given, which rendered similar data. Standard deviations reveal the quality of curve-fitting.

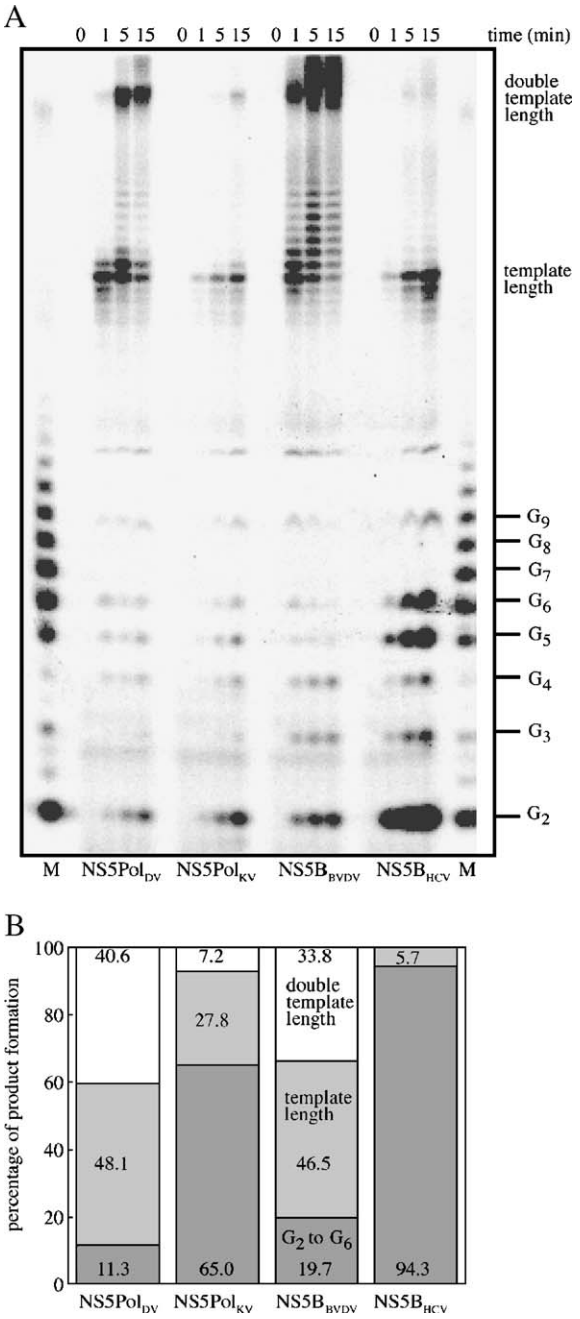

Fig. 7. De novo RNA synthesis by $NS5Pol_{DV}$, $NS5Pol_{KV}$, $NS5B_{BVDV}$ and $NS5B_{HCV}$ using an oligo(rC) RNA template. Reaction mixtures containing 400 nM enzyme, 10 μM oligo(rC) and 100 μM [α-^{32}P]-GTP were set up and processed as described under Materials and methods. Reaction time course was followed up to 15 min. (A) RNA products were resolved on a 14% polyacrylamide denaturating gel. M: Oligo(rG) RNA synthesized by T7 DdRp was used as RNA size marker. The identity of each band is indicated on the right. (B) Percentage of abortive, template length and double-template length products upon de novo RNA synthesis. Product bands were quantitated and the percentage of GMP incorporation in each product calculated from relative intensities of the corresponding band.

De novo initiation on homooligomeric RNA templates

In order to obtain information on putative rate-limiting steps within de novo initiation and elongation, reaction kinetics of RdRp domains $NS5Pol_{DV}$ and $NS5Pol_{KV}$ were followed using

an oligonucleotide containing 15 consecutive cytidines (oligo $(rC)_{15}$), and compared to the recombinant, single-domain RdRps of BVDV ($NS5B_{BVDV}$) and HCV ($NS5B_{HCV}$). We observe the accumulation of three types of products (Fig. 7A): (1) small products, i.e., G_2 to G_6, (2) template-size products and 3) long products that represent products around twice the size of the template, probably due to template-switching (Kim and Kao, 2001; Ranjith-Kumar et al., 2002b; Ranjith-Kumar et al., 2003). The accumulation of short products indicates rate-limiting steps for the subsequent phosphodiester bond formation marking the transition between initiation and elongation (Dutartre et al., 2005). Percentage of product formation was calculated, compared, and reported in Fig. 7B. For comparative purposes, we chose reaction mixtures from different time points (5 min for $NS5Pol_{DV}$ and $NS5B_{BVDV}$, 15 min for $NS5Pol_{KV}$ and 1 min for $NS5B_{HCV}$) giving to a similar overall GMP incorporation. $NS5Pol_{DV}$ produces mainly long products. The accumulation of shorter abortive products is low (11.3%). $NS5Pol_{KV}$ shows a considerable higher tendency to form short products representing 65.0% of total products. In the case of $NS5B_{BVDV}$ little accumulation of abortion products (19.7%) is observed. In contrast and as reported before (28), $NS5B_{HCV}$ appears rather distributive in that after 1 min, 94.3% of the products are abortive. Finally, some products are longer than template-size products by one to five nucleotides. They might have been generated by an intrinsic terminal nucleotide transferase activity, which has been reported for Flaviviridae RdRps (Ranjith-Kumar et al., 2001; Ranjith-Kumar et al., 2002b). The observation that the tendency to form theses products seems to be proportional to the tendency of template-switching, suggests that the formation of abortive products after template switching might also be responsible for the appearance of these product bands. $NS5Pol_{DV}$ and $NS5B_{BVDV}$ show a higher tendency to form these products than the other two *Flaviviridae* RdRps.

Discussion

The flavivirus replicative complex is made of several large, multi-domain enzymes that exhibit coordinated activities such RNA synthesis, RNA capping, helicase, and protease activities. Delineating individually active protein domains is one of the prerequisites to get access to structural and functional studies of the flavivirus replicative complex. In this study, we have delineated functional RdRp domains of 74 kDa of DV and WNV NS5. They were expressed in *E. coli* as soluble proteins, and purified in high yield without extensive loss due to protein degradation observed for full-length NS5 proteins (Fig. 2 and Table 1). The RdRp domains were active and showed the same enzymatic characteristics as their full-length counterparts (see below).

The RdRp domain includes the two NLS (Brooks et al., 2002) unique to flavivirus RdRps. A structural alignment of RdRp domains of the RNA viruses of *Cystiviridae* (PDB code 1hhs), *Reoviridae* (1muk), *Picornaviridae* (1ra6, 1xr7, 1wne), *Caliciviridae* (1khx, 1sh3), BVDV (1s48) and HCV (1c2p) using Multiprot (Shatsky et al., 2004) indicates that two helices corresponding to residues 350 to 390 within the NLSs of flavivirus NS5Pol are the two most N-terminal structural elements which are strictly conserved in all viral RdRp structures (indicated in Fig. 1). The two helices, predicted for flavivirus RdRps, form the central part of the flavivirus NLS. We therefore suggest that the NLS does not represent an inter-domain region as commonly believed (Brooks et al., 2002) but rather form an integral part of the RdRp domain. The preceding N-termini of RdRp domains form part of the fingertips, which provide a RdRp-typical bridge between fingers and thumb (Joyce and Steitz, 1995). They are structurally diverse. We propose that the putative interdomain region flavivirus NS5 might rather be situated within the limits of residues 265 to 310.

The purified RdRp domain of Dengue virus is active on a specific heteropolymeric template comprising elements of the 5′- and 3′-ends essential for efficient RNA synthesis (Ackermann and Padmanabhan, 2001; You and Padmanabhan, 1999). As reported by others (Ackermann and Padmanabhan, 2001; You and Padmanabhan, 1999), two kinds of product were generated, a hairpin product generated by a copy-back mechanism and the template-size product generated by de novo synthesis. Under the reaction conditions used in this study, the hairpin product represents around 80% of total product. Mg^{2+} ions or Mn^{2+} ions act as catalytic ions. At their optimal concentrations (4.5 mM for Mg^{2+}, 2 mM for Mn^{2+}), CMP-incorporation after 60 min was around 15-fold higher in presence of Mn^{2+} than in presence of Mg^{2+} (see Fig. 3). Thus, in our hands, Mn^{2+} is the preferred cation of DV RdRp.

Processive de novo RdRp activity could be monitored for all purified flavivirus RdRp domains and full-length proteins using the homopolymeric template poly(rC). This is in contrast to results obtained by Steffens et al. (1999) who found that $NS5_{WNV}$ is strictly dependent on the presence of a primer. The reason for this apparent discrepancy may lie in different experimental conditions. Steffens et al. (1999) used low GTP concentration and Mg^{2+} as the sole catalytic metal ion. We observe RNA synthesis exclusively when Mn^{2+} ions are present in the reaction mixture. Mn^{2+} ions have been shown to exert a variety of effects on polymerase activities. They may (1) modulate overall activity (Arnold et al., 1999; Blanca et al., 2003; Ranjith-Kumar et al., 2002b), (2) change the ratio of de novo initiation as compared to 3′ elongation (Ranjith-Kumar et al., 2002b), (3) influence additional activities as terminal nucleotide transferase activities (Ranjith-Kumar et al., 2001, 2002b) and (4) change specificity for template and nucleotides (Pinto et al., 1979; Ranjith-Kumar et al., 2002a; Tabor and Richardson, 1989). Interestingly, for three *Flaviviridae* RdRps different effects were reported using a template that allows de novo initiation and 3′ elongation at the same time (Ranjith-Kumar et al., 2002b). When 2 mM Mg^{2+} or Mn^{2+} were compared, overall activity in the presence of Mn^{2+} was either higher, unchanged, or lower. Additionally, it was reported for $NS5B_{HCV}$ and $NS5B_{BVDV}$ that the presence of 1 mM Mn^{2+} in addition to 4 mM Mg^{2+} relaxed the recognition stringency of the initiating nucleotide (Ranjith-Kumar et al., 2002a). In presence of Mn^{2+}, the K_m of the initiating nucleotide GTP decreased from 103 to 3 μM for $NS5B_{HCV}$ and from 168 to

24 μM for $NS5B_{BVDV}$. These factors, in combination with the observed activation of Dengue virus RdRp by Mn^{2+} (see above) might contribute to the Mn^{2+}-dependent de novo activity of flavivirus RdRps on poly(rC) measured in our study. Mn^{2+} ions seem to have an activating effect on flavivirus RdRps regarding overall activity and de novo initiation with GTP acting as initiating nucleotide.

Our results indicate that flavivirus RdRps can use GTP as initiating nucleotide even though adenine is the first nucleotide of both (+) and (−) strand of flavivirus RNA. Using poly(rU), $NS5_{DV}$ and $NS5Pol_{DV}$ exhibit ~20% of the activity obtained using poly(rC), whereas the WNV enzymes do not exhibit any activity. This might suggest that flavivirus RdRps prefer GTP as initiating nucleotide. Note that when activity of $NS5_{DV}$ was measured on specific subgenomic templates (Nomaguchi et al., 2003), an unusually high GTP concentration was necessary for de novo RNA synthesis leading to the hypothesis that GTP might be the actual initiating nucleotide in vivo. Another possibility is that GTP plays a special role in the formation of the de novo initiation complex. For *Flaviviridae* NS5B RdRps, GTP is proposed to provide a de novo initiation platform (Ferron et al., 2005a) being positioned at an additional binding site defined by motif E (Fig. 1) next to the active site. This additional binding site had been identified in the structure of $NS5B_{BVDV}$ (Choi et al., 2004). It might exist as well on flavivirus RdRps given that motif E is conserved within the *Flaviviridae* RdRps (Fig. 1).

Using poly(rC), we were able to determine K_m values of GTP for de novo RNA synthesis for all flavivirus RdRp constructs (Table 2). This had not been possible for de novo synthesis by $NS5_{DV}$ using a minigenomic RNA template (Nomaguchi et al., 2003) because no regular Michaelis–Menten kinetics could be observed. It is not the case for flavivirus RdRps on poly(rC) (Fig. 6). Data fitted well to Hill equations that provide $K_{0.5}$ values, which correspond to K_m values of the classic Michaelis–Menten equation and will be denominated as such in the following discussion. Interestingly, we measured different K_m (GTP) values for DV and WNV RdRps. For DV RdRps, K_m (GTP) is close to 20 μM whereas it is 5- to 8-fold higher for WNV RdRps. Both values can be considered high in comparison to the measured K_m(GTP) value of 0.37 μM for $NS5_{DV}$ upon elongation on a Dengue minigenomic template (Nomaguchi et al., 2003). These high K_m(GTP) values may correspond to the general observation that initiating nucleotides show high K_m values even in presence of Mn^{2+} ions (Dutartre et al., 2005; Luo et al., 2000; Ranjith-Kumar et al., 2002a). In contrast to the clear difference of the K_m(GTP) values of DV and WNV RdRps, we determined similar Hill coefficients for DV and WNV RdRps. Hill coefficients with a value greater than 1 as we have observed for GTP may indicate (1) the existence of additional binding sites different from the NTP incorporation site in the active centre (binding cooperativity), (2) the existence of one binding site but different enzyme conformations with different catalytic properties that are not in equilibrium (kinetic cooperativity (Cornish-Bowden and Cardenas, 1987)) and (3) the artifactual existence of additional binding sites in the context of the experimental system used. We think we can discard the possibility of an artifact given the fact that a special behavior of GTP in comparison to other NTPs had been observed by others (Nomaguchi et al., 2003) using a Dengue minigenome template. Future binding experiments and additional experiments exploring the role of GTP in other experimental systems (poly(rU), RNA minigenome or other heteropolymeric templates) might enable us to distinguish between the first and the second case. If the first interpretation holds true, an additional binding site could be a site next to motif E involved in the formation of an initiation platform (Ferron et al., 2005a), or it could correspond to the site that has been identified for $NS5B_{HCV}$ (Bressanelli et al., 2002). The comparison of the data obtained for RdRp domains and full-length proteins (Table 2) indicate that the GTP binding site on the MTase domain (K_D(GTP) for $NS5MTase_{DV}$ 58 μM (Egloff et al., 2002)) does not interfere with the polymerase activity. Similarly, for other characteristics tested (alternative homopolymeric templates and influence of non-ionic detergents and BSA), we did not detect any significant difference between RdRp domains and full-length proteins. The same applies to the obtained k_{cat} values of the WNV proteins. The k_{cat} values of $NS5_{DV}$ being lower than for $NS5Pol_{DV}$ can be explained by the lower purity of the enzyme preparation (see Fig. 2C) causing an overestimation of enzyme concentration by measuring absorption at 280 nm., Our results thus indicate that, although covalently linked, the two domains of NS5 responsible for RNA capping and RNA synthesis function in a catalytically autonomous manner.

De novo RNA synthesis on $oligo(rC)_{15}$ was analyzed to detect rate-limiting steps that may indicate possible conformational changes involved in the transition from initiation to elongation. Since we did not observe any differences in the enzymatic characteristics of flavivirus RdRp domains and full-length proteins, we compared $NS5Pol_{DV}$, $NS5Pol_{KV}$ and the single-domain RdRps $NS5B_{BVDV}$ and $NS5B_{HCV}$ (Fig. 7). In the case of $NS5B_{HCV}$ the existence of several distinct steps of RNA synthesis have been identified: 1) a non-rate limiting step of initiation (formation of G_2), 2) a rate-limiting step (change of conformation?) of formation of G_3, 3) the formation of G_4, 4) a rate-limiting step (change of conformation?) of formation of G_5 and G_6 and 5) the final elongation of the G_6 product to longer products (Dutartre et al., 2005). Step 1) may be regarded as initiation, steps 2) to 4) as transition, and step 5) as elongation. In the case of HCV NS5B, the allosteric GTP binding site (Bressanelli et al., 2002) seems to be involved in the conformational change occurring during step 4) (Dutartre et al., 2005). This step might involve the "flap" (see Fig. 1), moving away from the active site allowing subsequently processive RNA synthesis. As illustrated in Fig. 7, the results for $NS5B_{HCV}$ follow the pattern described above (94.3% abortive products). For flavivirus NS5Pol we observed less accumulation of abortive products (11.3% for $NS5Pol_{DV}$ and 65.0% for $NS5Pol_{KV}$). This might indicate that either there is no putative "flap"-like structural element, or it exists but the necessary conformational change is less rate limiting. For $NS5B_{BVDV}$ the percentage of short abortive products is as low as for $NS5Pol_{DV}$. The structure of $NS5B_{BVDV}$ (Choi et al., 2004) revealed that a "flap"-like structural element exists although

adopting a different fold and positioning in relation to the active site than that of $NS5B_{HCV}$ (see Fig. 1). It is reasonable to expect the existence of such a structural element for flavivirus RdRps as well. Considering the sequence conservation of flavivirus RdRp domains, DV and WNV RdRps should have a very similar structure. The observed difference between $NS5Pol_{DV}$ and $NS5Pol_{KV}$ seems rather to express a variation in conformational flexibility of structurally similar elements. KV RdRP seems to approach the limited flexibility of HCV RdRp. In the absence of atomic resolution structural data, it is difficult to speculate further on this putative "flap" given the low degree of sequence conservation of the flavivirus NS5B with both $NS5B_{HCV}$ and $NS5B_{BVDV}$. Regarding their mode of transition from initiation to elongation observed here, flavivirus RdRps seem to be more similar to the pestivirus RdRp, which shows a higher conformational flexibility than the hepacivirus RdRp.

Several distinct template-size products in Fig. 7 indicate that $NS5Pol_{DV}$ acts as a terminal nucleotide transferase or is prone to template slippage. Later during the time course of RNA synthesis, even longer products are produced to a larger extent (40.6% after 5 min). They have around twice the size of the template and might thus be generated by template switching when the polymerase reaches the end of a first template. Both activities can be observed for $NS5B_{KV}$ in Fig. 7 albeit to a far lesser extent than for $NS5Pol_{DV}$. Terminal transferase activity and template switching have been described for pestivirus and hepacivirus RdRps on heteropolymeric templates (Kim and Kao, 2001; Ranjith-Kumar et al., 2001, 2002a, 2002b, 2003). In our experiments, the terminal transferase activity and the template-switching tendency of $NS5B_{BVDV}$ are by far more important than for $NS5B_{HCV}$ as observed by others on heteropolymeric templates (Ranjith-Kumar et al., 2002a, 2002b). Here again, DV RdRp RdRps seem to be more similar to the pestivirus than to the hepacivirus RdRp.

In summary, this study contributes to the in-depth characterization of flavivirus RdRp, which has somehow lagged behind that of pestivirus and hepacivirus RdRps. The flavivirus RdRp domain described here is active on specific heteropolymeric and homopolymeric templates. It is able to conduct de novo RNA synthesis. The MTase domain does not influence significantly the polymerase activity. Thus, the physical dissociation of the two activities of NS5 does allow meaningful functional and inhibition studies. Sequence differences between flavivirus RdRp domains are reflected into the K_m for the (in vitro) initiating GTP, higher for WNV RdRps than for DV RdRps. Furthermore, the differences between WNV and DV RdRp observed for the transition between initiation and elongation of de novo RNA synthesis indicate a lower degree of conformational flexibility for WNV RdRp. Both enzymes displayed a Hill coefficient higher than 1, suggesting the existence of an additional GTP binding site and positive cooperativity. In the absence of structural data, it would be interesting to design experiments to address the question of multiple, non-catalytic flavivirus RdRp GTP binding sites. Last, in linking biochemical data indicating conformational flexibility to structural determinants, our work provides an interesting start to studies beyond drug-design, such as template switching and RdRp-mediated recombination in *Flaviviridae*.

Materials and methods

Cloning

RT-PCR products for generating the expression constructs of $NS5_{DV}$ and $NS5Pol_{DV}$ (DV serotype 2, New Guinea C strain) were kindly provided by H. Toulou, Unité de Virologie Tropicale, Institut de Médecine Tropicale du Service de Santé des Armées (IMTSSA), Marseille, France. The coding sequences for DV RdRp domain and full-length NS5 were cloned into expression plasmid pQE30 (Qiagen) adding a His_6-tag at the N-terminus of the expressed proteins. WNV strain IS-98-ST1 (GenBank accession number AF 481864), a recent pathogenic isolate used as a viral model for West Nile encephalitis in the Old World (Lucas et al., 2004), was propagated in mosquito *Aedes pseudoscutellaris* AP61 cell monolayers. The genomic RNA of WNV was extracted from sucrose-gradient purified IS-98-ST1 virions and reverse transcribed using Titan One-Step RT-PCR kit (Roche Molecular Biochemicals). An RT-PCR fragment encoding NS5 was generated using the forward primer 5′-CCAGGACTACA-TATGGGTGGGGCAAAAGGACGCACCTTGG-3′ and the reverse primer 5′-CTAATAAAACTAAGCTTTTATGCA-TACTTATATTGT-3′. Plasmid pBSNS5His3′UTR (A. Khromykh, unpublished data) which contained the gene coding for NS5 of the Kunjin subtype of WNV (strain MRM61C) was used for the generation of the expression vectors for $NS5_{KV}$ and $NS5Pol_{KV}$. All the WNV coding sequences for RdRp domains and full-length proteins were cloned into vector pDest14 from the Gateway system (Life technologies) equally adding a His_6-tag at the N-terminus.

Protein expression and purification

DV constructs in pQE30 plasmids were expressed in BL21 [pDNAy] or Rosetta[pLacI] (Novagen). Constructions in pDest14 plasmids were expressed in Rosetta[pLysS] (Novagen). Expressions for all proteins were carried out overnight at 17 °C after induction with 50 μM IPTG, addition of 2% EtOH and a cold shock (30 min at 4 °C). Sonication was done in 50 mM sodium phosphate lysis buffer, pH 7.5, 300 mM NaCl, 10% glycerol and 5 mM $MgCl_2$ (10 ml of this lysis buffer for 3.6 g cell pellet) in the presence of DNase I, phenylmethylsulfonyl fluoride (PMSF), protease inhibitor cocktail (SIGMA) and lysozyme after 30 min incubation at 4 °C. For WNV proteins 50 mM Tris buffer with the same pH and composition of salts and additives could be used giving similar results. After centrifugation the soluble fraction was incubated in batch with TALON metal-affinity resin (Clontech), washed twice with binding buffer and once with binding buffer plus 20 mM imidazole. Protein fractions were then eluted with binding buffer containing 500 mM imidazole. After dialysis (10 mM Tris buffer, pH 7.5, 300 mM NaCl, 5 mM $MgCl_2$, 20% glycerol) proteins were diluted with the same volume of this buffer

without NaCl, bound to Heparin-sepharose 6 fast flow (Amersham-Biosciences) and incubated for 30 min at 4 °C. They were then eluted with the binding buffer containing 600 mM NaCl. Alternatively, gel filtration was used as a second purification step using a Superdex 200 HR 30/11 column (Amersham-Biosciences) and the dialysis buffer. Proteins showed ca. 98% (RdRp domains) and 85% (full-length proteins) purity and were stored in 10 mM Tris, pH 7.5, 300 mM NaCl, 40% glycerol at −20 °C. Under this condition they displayed long storage stability. $NS5B_{HCV}$ (55 C-terminal residues deleted) was expressed and purified as previously described (Dutartre et al., 2005). The $NS5B_{BVDV}$ expression plasmid pET28a[NS5BΔCT24] was kindly provided by V. Lai and Z. Hong (Ribapharm, Costa Mesa, USA). For expression and purification of $NS5B_{BVDV}$ (24 C-terminal residues deleted), published protocols were followed (Lai et al., 1999).

RdRp activity tests, reagents and detection methods

Homopolymeric RNA templates poly(rC), poly(rA) and poly (rU) were obtained from Amersham-Biosciences. RNA oligonucleotides $oligo(rC)_{15}$ were obtained from Dharmacon. Labeled nucleotides were purchased from Amersham-Bioscience. RNA molecular weight marker was purchased from Ambion. DNA oligonucleotides were obtained from Invitrogen.

RdRp activity tests monitored by filter-binding and liquid scintillation counting were stopped after given times by spotting aliquots onto DE-81 filter discs (Whatman) pre-treated with equal volumes of 50 mM EDTA. When [^{32}P]-labeled NTPs were used, filters were pre-treated with equal volumes of EDTA and 50 mM K_2HPO_4, pH 7.4. Filter discs were dried and washed three times with 0.3 M ammonium formate, pH 8.0, and once with ethanol and dried. Liquid scintillation fluid was added and incorporation was measured in counts per minute (cpm) by using a Wallac MicroBeta TriLux Liquid Scintillation Counter.

RdRp activity tests monitored by PAGE were quenched by adding formamide/EDTA gel-loading buffer. Reaction products were separated using sequencing gels of either 14% acrylamide-bisacrylamide (19:1), 7 M Urea with TTE buffer (89 mM Tris pH 8.0, 28 mM taurine (2-aminoethanesulfonic acid), 0.5 mM EDTA) or of 4% acrylamide-bisacrylamide (19:1), 7 M Urea with TBE buffer (89 mM Tris pH 8.0, 89 mM boric acid, 2 mM EDTA). RNA product bands were visualized using photo-stimulated plates and the Fluorescent Image Analyzer FLA3000 (Fuji) and quantified using Image Gauge (Fuji).

$NS5Pol_{DV}$ RdRp activity test on heteropolymeric template (Dengue minigenome)

Dengue minigenome (DMG) consists of the first 224 nucleotides of the 5′ end and 492 last nucleotides of the 3′ end of genomic RNA. It was obtained by three PCR reactions from a plasmid containing the complete genomic sequence of Dengue 2 (New Guinea C) kindly provided by Barry Falgout, Division of Viral Products, Center of Biologics Evaluation and Research, Food and Drug Administration, Rockville, USA. The final PCR product was cloned into the *Hin*dIII/*Xba*I sites of plasmid pUC18. The T7 DNA-dependent RNA polymerase (T7 DdRp) promoter sequence and three guanines TAATACGACTCACTATAGGG were added just upstream the DMG 5′. For the PCR reaction yielding the DNA template for in vitro transcription, primer 5′-AAGCTTTAATACGACTCACTATA-3′ and reverse primer 5′-AGAACCTGTTGATTCAACAG-3′ were used providing the precise 3′ end of genomic Dengue RNA. The RNA template was then generated by in vitro transcription with T7 DdRp using 5 μg of PCR product as a template in reactions made of 50 μl T7 DdRp buffer (40 mM Tris HCl pH 7.5, 6 mM $MgCl_2$, 2 mM spermidine, 10 mM DTT) containing 2 mM NTPs, 1 μl SUPERase●In (Ambion) and 4 μg recombinant T7 DdRp. Reactions were incubated for 3 *h* at 37 °C and then stopped by RNase-free DNase I treatment. RNA was purified by MEGAclear (Ambion).

Reactions analyzed by PAGE (4%, buffer TBE, see above) were performed in flavivirus RdRp buffer (50 mM HEPES pH 8.0, 10 mM KCl, 5 mM $MnCl_2$, 5 mM $MgCl_2$, 10 mM DTT), using 200 nM RNA template, 500 μM ATP, UTP and GTP, 10 μM CTP (0.1 μCi [α-^{32}P]-CTP per μl reaction volume) and the given amount of $NS5Pol_{DV}$. Reactions were allowed to proceed for 60 min at 30 °C.

Reactions analyzed by filter-binding assays were run under the same conditions except for 100 nM RNA template, 200 nM $NS5Pol_{DV}$ and variable amounts (between 0 and 10 mM) of $MgCl_2$ or $MnCl_2$.

Flavivirus RdRp test on homopolymeric templates

RdRp activity tests of NS5 proteins monitored by filter-binding and liquid scintillation counting were run in flavivirus RdRp buffer (see above) containing 1 μM homopolymeric RNA template, RdRps at concentrations given in figure legends and 10 μM (DV assay) or 100 μM (WNV assay) GTP (0.01 to 0.05 μCi [^{3}H]-GTP per μl, 5.20 Ci/mmol), if not stated otherwise. Variations include addition of 4 μM rGG primer, 37 nM *E. coli* RNA polymerase (USBiochemicals) or *E. coli* DdRp inhibitor rifampicin (Sigma) at 1.3 ng/μl. Reactions were initiated by the addition of a premix of GTP, Mn^{2+} and Mg^{2+}, incubated at 30 °C. Data of complete reaction time courses and GTP concentration dependence of initial velocities were fitted using Kaleidagraph (Synergy Software) and equations indicated in Results.

Reactions analyzed by PAGE (14%, buffer TTE, see above) were done under the same conditions using 10 μM or 100 μM GTP (0.1 μCi [α-^{32}P]-GTP per μl reaction volume) and 1 μM poly(rC) or 10 μM $oligo(rC)_{15}$ (see figure legends). Template concentrations refer to molar concentration of the polymer (around 500 nt) or oligomer. For $NS5B_{BVDV}$ and $NS5B_{HCV}$, RdRp buffer was supplemented with 0.5% non-ionic detergent Igepal CA630. Oligo(rG) RNA weight marker was synthesized using T7 DdRp and DNA oligonucleotide templates. For this purpose, reactions were performed in 10 μl T7 DdRp buffer (see above) at 37 °C for 10 min, using 50 pmol of DNA oligonucleotide (5′-TTTTTTTTTTTTTTTTTTTTTCCTATAGTGAGTCGTATTA-3′ or 5′-TTTTTTTTTTTTTTTTTTCCCCCTATAGTGAGTCGTATTA-3′) template annealed to

the T7 primer (5′-AAGCTTTAATACGACTCACTATA-3′) and 10 μM GTP (1 μCi [α-^{32}P]-GTP). Reactions were initiated by the addition of 1 μg of recombinant T7 DdRp and treated afterwards with RNase-free DNase I for 15 min at 37 °C.

Acknowledgments

We thank Dr. Hugues Tolou for continuous encouragements and support, Drs. Maria Luz Cárdenas and Athel Cornish-Bowden for their most valuable advice on steady-state kinetics and critical revision of the manuscript as well as Drs. Subhash Vasudevan and Holly Murphy for both critical reading and improving the English of the manuscript. This investigation was supported in part by the French Ministry Program "Maladies Infectieuses", a grant from the Direction Générales des Armées, and in part by the EU-FP5 program "Flavitherapeutics" (QLK3-CT-2001-00506), and subsequently the EU-FP6 VIZIER program (LSHG-CT-2004-511960). D.B. was supported by a pre-doctoral fellowship from the Direction Générales des Armées and the Fondation pour la Recherche Medicale.

References

Ackermann, M., Padmanabhan, R., 2001. De novo synthesis of RNA by the dengue virus RNA-dependent RNA polymerase exhibits temperature dependence at the initiation but not elongation phase. J. Biol. Chem. 276 (43), 39926–39937.

Ago, H., Adachi, T., Yoshida, A., Yamamoto, M., Habuka, N., Yatsunami, K., Miyano, M., 1999. Crystal structure of the RNA-dependent RNA polymerase of hepatitis C virus. Structure Fold Des. 7 (11), 1417–1426.

Arnold, J.J., Ghosh, S.K., Cameron, C.E., 1999. Poliovirus RNA-dependent RNA polymerase (3D(pol)). Divalent cation modulation of primer, template, and nucleotide selection. J. Biol. Chem. 274 (52), 37060–37069.

Benarroch, D., Egloff, M.P., Mulard, L., Guerreiro, C., Romette, J.L., Canard, B., 2004. A structural basis for the inhibition of the NS5 dengue virus mRNA 2′-O-methyltransferase domain by ribavirin 5′-triphosphate. J. Biol. Chem. 279 (34), 35638–35643.

Blanca, G., Shevelev, I., Ramadan, K., Villani, G., Spadari, S., Hubscher, U., Maga, G., 2003. Human DNA polymerase lambda diverged in evolution from DNA polymerase beta toward specific Mn(++) dependence: a kinetic and thermodynamic study. Biochemistry 42 (24), 7467–7476.

Bressanelli, S., Tomei, L., Roussel, A., Incitti, I., Vitale, R.L., Mathieu, M., De Francesco, R., Rey, F.A., 1999. Crystal structure of the RNA-dependent RNA polymerase of hepatitis C virus. Proc. Natl. Acad. Sci. U.S.A. 96 (23), 13034–13039.

Bressanelli, S., Tomei, L., Rey, F.A., De Francesco, R., 2002. Structural analysis of the hepatitis C virus RNA polymerase in complex with ribonucleotides. J. Virol. 76 (7), 3482–3492.

Brooks, A.J., Johansson, M., John, A.V., Xu, Y., Jans, D.A., Vasudevan, S.G., 2002. The interdomain region of dengue NS5 protein that binds to the viral helicase NS3 contains independently functional importin beta 1 and importin alpha/beta-recognized nuclear localization signals. J. Biol. Chem. 277 (39), 36399–36407.

Choi, K.H., Groarke, J.M., Young, D.C., Kuhn, R.J., Smith, J.L., Pevear, D.C., Rossmann, M.G., 2004. The structure of the RNA-dependent RNA polymerase from bovine viral diarrhea virus establishes the role of GTP in de novo initiation. Proc. Natl. Acad. Sci. U.S.A. 101 (13), 4425–4430.

Cornish-Bowden, A., Cardenas, M.L., 1987. Co-operativity in monomeric enzymes. J. Theor. Biol. 124 (1), 1–23.

Dutartre, H., Boretto, J., Guillemot, J.C., Canard, B., 2005. A relaxed discrimination of 2′-O-methyl-GTP relative to GTP between de novo and elongative RNA synthesis by the hepatitis C RNA-dependent RNA polymerase NS5B. J. Biol. Chem. 280 (8), 6359–6368.

Egloff, M.P., Benarroch, D., Selisko, B., Romette, J.L., Canard, B., 2002. An RNA cap (nucleoside-2′-O-)-methyltransferase in the flavivirus RNA polymerase NS5: crystal structure and functional characterization. EMBO J. 21 (11), 2757–2768.

Ferron, F., Bussetta, C., Dutartre, H., Canard, B., 2005a. The modeled structure of the RNA dependent RNA polymerase of GBV-C Virus suggests a role for motif E in Flaviviridae RNA polymerases. BMC Bioinformatics 6 (1), 255.

Ferron, F., Rancurel, C., Longhi, S., Cambillau, C., Henrissat, B., Canard, B., 2005b. VaZyMolO: a tool to define and classify modularity in viral proteins. J. Gen. Virol. 86 (Pt 3), 743–749.

Galtier, N., Gouy, M., Gautier, C., 1996. SEAVIEW and PHYLO_WIN: two graphic tools for sequence alignment and molecular phylogeny. Comput. Appl. Biosci. 12 (6), 543–548.

Gouet, P., Robert, X., Courcelle, E., 2003. ESPript/ENDscript: extracting and rendering sequence and 3D information from atomic structures of proteins. Nucleic Acids Res. 31 (13), 3320–3323.

Guyatt, K.J., Westaway, E.G., Khromykh, A.A., 2001. Expression and purification of enzymatically active recombinant RNA-dependent RNA polymerase (NS5) of the flavivirus Kunjin. J. Virol. Methods 92 (1), 37–44.

Guzman, M.G., Kouri, G., 2002. Dengue: an update. Lancet Infect. Dis. 2 (1), 33–42.

Hall, R.A., Khromykh, A.A., 2004. West Nile virus vaccines. Expert Opin. Biol. Ther. 4 (8), 1295–1305.

Hall, R.A., Broom, A.K., Smith, D.W., Mackenzie, J.S., 2002. The ecology and epidemiology of Kunjin virus. Curr. Top. Microbiol. Immunol. 267, 253–269.

Hall, R.A., Nisbet, D.J., Pham, K.B., Pyke, A.T., Smith, G.A., Khromykh, A.A., 2003. DNA vaccine coding for the full-length infectious Kunjin virus RNA protects mice against the New York strain of West Nile virus. Proc. Natl. Acad. Sci. U.S.A. 100 (18), 10460–10464.

Joyce, C.M., Steitz, T.A., 1995. Polymerase structures and function: variations on a theme? J. Bacteriol. 177 (22), 6321–6329.

Kao, C.C., Singh, P., Ecker, D.J., 2001. De novo initiation of viral RNA-dependent RNA synthesis. Virology 287 (2), 251–260.

Kim, M.J., Kao, C., 2001. Factors regulating template switch in vitro by viral RNA-dependent RNA polymerases: implications for RNA-RNA recombination. Proc. Natl. Acad. Sci. U.S.A. 98 (9), 4972–4977.

Koonin, E.V., 1991. The phylogeny of RNA-dependent RNA polymerases of positive-strand RNA viruses. J. Gen. Virol. 72 (Pt 9), 2197–2206.

Lai, V.C., Kao, C.C., Ferrari, E., Park, J., Uss, A.S., Wright-Minogue, J., Hong, Z., Lau, J.Y., 1999. Mutational analysis of bovine viral diarrhea virus RNA-dependent RNA polymerase. J. Virol. 73 (12), 10129–10136.

Lanciotti, R.S., Ebel, G.D., Deubel, V., Kerst, A.J., Murri, S., Meyer, R., Bowen, M., McKinney, N., Morrill, W.E., Crabtree, M.B., Kramer, L.D., Roehrig, J.T., 2002. Complete genome sequences and phylogenetic analysis of West Nile virus strains isolated from the United States, Europe, and the Middle East. Virology 298 (1), 96–105.

Leipe, D.D., Aravind, L., Koonin, E.V., 1999. Did DNA replication evolve twice independently? Nucleic Acids Res. 27 (17), 3389–3401.

Lesburg, C.A., Cable, M.B., Ferrari, E., Hong, Z., Mannarino, A.F., Weber, P.C., 1999. Crystal structure of the RNA-dependent RNA polymerase from hepatitis C virus reveals a fully encircled active site. Nat. Struct. Biol. 6 (10), 937–943.

Lucas, M., Frenkiel, M.P., Mashimo, T., Guenet, J.L., Deubel, V., Despres, P., Ceccaldi, P.E., 2004. The Israeli strain IS-98-ST1 of West Nile virus as viral model for West Nile encephalitis in the Old World. Virol. J. 1 (1), 9.

Luo, G., Hamatake, R.K., Mathis, D.M., Racela, J., Rigat, K.L., Lemm, J., Colonno, R.J., 2000. De novo initiation of RNA synthesis by the RNA-dependent RNA polymerase (NS5B) of hepatitis C virus. J. Virol. 74 (2), 851–863.

Mackenzie, J.S., Gubler, D.J., Petersen, L.R., 2004. Emerging flaviviruses: the spread and resurgence of Japanese encephalitis, West Nile and dengue viruses. Nat. Med. 10 (12 Suppl), S98–S109.

Murzin, A.G., Brenner, S.E., Hubbard, T., Chothia, C., 1995. SCOP: a structural classification of proteins database for the investigation of sequences and structures. J. Mol. Biol. 247 (4), 536–540.

Nomaguchi, M., Ackermann, M., Yon, C., You, S., Padmanabhan, R., 2003. De novo synthesis of negative-strand RNA by Dengue virus RNA-dependent RNA polymerase in vitro: nucleotide, primer, and template parameters. J. Virol. 77 (16), 8831–8842.

Nomaguchi, M., Teramoto, T., Yu, L., Markoff, L., Padmanabhan, R., 2004. Requirements for West Nile virus (−)- and (+)-strand subgenomic RNA synthesis in vitro by the viral RNA-dependent RNA polymerase expressed in *Escherichia coli*. J. Biol. Chem. 279 (13), 12141–12151.

O'Reilly, E.K., Kao, C.C., 1998. Analysis of RNA-dependent RNA polymerase structure and function as guided by known polymerase structures and computer predictions of secondary structure. Virology 252 (2), 287–303.

Pinto, D., Sarocchi-Landousy, M.T., Guschlbauer, W., 1979. 2′-Deoxy-2′-fluorouridine-5′-triphosphates: a possible substrate for *E. coli* RNA polymerase. Nucleic Acids Res. 6 (3), 1041–1048.

Pugachev, K.V., Guirakhoo, F., Trent, D.W., Monath, T.P., 2003. Traditional and novel approaches to flavivirus vaccines. Int. J. Parasitol. 33 (5–6), 567–582.

Ranjith-Kumar, C.T., Gajewski, J., Gutshall, L., Maley, D., Sarisky, R.T., Kao, C.C., 2001. Terminal nucleotidyl transferase activity of recombinant Flaviviridae RNA-dependent RNA polymerases: implication for viral RNA synthesis. J. Virol. 75 (18), 8615–8623.

Ranjith-Kumar, C.T., Gutshall, L., Kim, M.J., Sarisky, R.T., Kao, C.C., 2002a. Requirements for de novo initiation of RNA synthesis by recombinant flaviviral RNA-dependent RNA polymerases. J. Virol. 76 (24), 12526–12536.

Ranjith-Kumar, C.T., Kim, Y.C., Gutshall, L., Silverman, C., Khandekar, S., Sarisky, R.T., Kao, C.C., 2002b. Mechanism of de novo initiation by the hepatitis C virus RNA-dependent RNA polymerase: role of divalent metals. J. Virol. 76 (24), 12513–12525.

Ranjith-Kumar, C.T., Santos, J.L., Gutshall, L.L., Johnston, V.K., Lin-Goerke, J., Kim, M.J., Porter, D.J., Maley, D., Greenwood, C., Earnshaw, D.L., Baker, A., Gu, B., Silverman, C., Sarisky, R.T., Kao, C., 2003. Enzymatic activities of the GB virus-B RNA-dependent RNA polymerase. Virology 312 (2), 270–280.

Roehrig, J.T., Staudinger, L.A., Hunt, A.R., Mathews, J.H., Blair, C.D., 2001. Antibody prophylaxis and therapy for flavivirus encephalitis infections. Ann. N.Y. Acad. Sci. 951, 286–297.

Rost, B., 1996. PHD: predicting one-dimensional protein structure by profile-based neural networks. Methods Enzymol. 266, 525–539.

Scherret, J.H., Poidinger, M., Mackenzie, J.S., Broom, A.K., Deubel, V., Lipkin, W.I., Briese, T., Gould, E.A., Hall, R.A., 2001. The relationships between West Nile and Kunjin viruses. Emerg. Infect. Dis. 7 (4), 697–705.

Shatsky, M., Nussinov, R., Wolfson, H.J., 2004. A method for simultaneous alignment of multiple protein structures. Proteins 56 (1), 143–156.

Steffens, S., Thiel, H.J., Behrens, S.E., 1999. The RNA-dependent RNA polymerases of different members of the family Flaviviridae exhibit similar properties in vitro. J. Gen. Virol. 80 (Pt 10), 2583–2590.

Tabor, S., Richardson, C.C., 1989. Effect of manganese ions on the incorporation of dideoxynucleotides by bacteriophage T7 DNA polymerase and *Escherichia coli* DNA polymerase I. Proc. Natl. Acad. Sci. U.S.A. 86 (11), 4076–4080.

Tan, B.H., Fu, J., Sugrue, R.J., Yap, E.H., Chan, Y.C., Tan, Y.H., 1996. Recombinant dengue type 1 virus NS5 protein expressed in *Escherichia coli* exhibits RNA-dependent RNA polymerase activity. Virology 216 (2), 317–325.

You, S., Padmanabhan, R., 1999. A novel in vitro replication system for Dengue virus. Initiation of RNA synthesis at the 3′-end of exogenous viral RNA templates requires 5′- and 3′-terminal complementary sequence motifs of the viral RNA. J. Biol. Chem. 274 (47), 33714–33722.